Eur Biophys J (2006) 35: 162–169
DOI 10.1007/s00249-005-0017-7

ARTICLE

**Karthikan Rajagopal · Bulent Ozbas · Darrin J. Pochan
Joel P. Schneider**

Probing the importance of lateral hydrophobic association in self-assembling peptide hydrogelators

Received: 21 May 2005 / Revised: 5 August 2005 / Accepted: 12 August 2005 / Published online: 8 November 2005

Abstract A class of peptides has been designed whose ability to self-assemble into hydrogel is dependent on their conformationally folded state. Under unfolding conditions aqueous peptide solutions are freely flowing having the viscosity of water. When folding is triggered by external stimuli, peptides adopt a β-hairpin conformation that self-assembles into a highly crosslinked network of fibrils affording mechanically rigid hydrogels. MAX 1, a 20 residue, amphiphilic hairpin self-assembles via a mechanism which entails both lateral and facial self-assembly events to form a network of fibrils whose local structure consists of a bilayer of hairpins hydrogen bonded in the direction of fibril growth. Lateral self-assembly along the long axis of the fibril is mainly facilitated by intermolecular hydrogen bonding between the strands of distinct hairpins and the formation of hydrophobic contacts between residue side chains of laterally associating hairpins. Facial assembly is driven by the hydrophobic collapse of the valine-rich faces of the amphiphilic hairpins affording a bilayer laminate. The importance of forming lateral hydrophobic contacts during hairpin self-assembly and the relative contribution these interactions have towards nano-scale morphology and material rigidity is probed via the study of: MAX1, a hairpin designed to exploit lateral hydrophobic interactions; MAX 4, a peptide with reduced ability to form these interactions; and MAX5, a control peptide. CD spectroscopy and rheological experiments suggest that the formation of lateral hydrophobic interactions aids the kinetics of assembly and contributes to the mechanical rigidity of the hydrogel. Transmission electron microscopy (TEM) shows that these interactions play an essential role in the self-assembly process leading to distinct nano-scale morphologies.

Keywords Peptide · Self-assembly · Hydrogel · Tissue engineering · Design · Viscoelastic

Electronic Supplementary Material Supplementary material is available for this article at http://dx.doi.org/10.1007/s00249-005-0017-7 and is accessible for authorized users.

K. Rajagopal · J. P. Schneider (✉)
Department of Chemistry and Biochemistry,
University of Delaware, Newark, DE 19716, USA
E-mail: schneijp@udel.edu
Tel.: +1-302-8313024

B. Ozbas · D. J. Pochan
Materials Science and Engineering Department,
Delaware Biotechnology Institute, University of Delaware,
Newark, DE 19716, USA
Tel.: +1-302-8313569

Introduction

Hydrogels are heavily hydrated materials finding use in tissue regeneration efforts (Lee and Mooney 2001; Rajagopal and Schneider 2004). The design of "smart" peptides (Aggeli et al. 1997; Collier et al. 2001; Holmes 2002; Kretsinger et al. 2005; Zhang et al. 1995) that undergo solution-hydrogel phase transitions in response to biological cues may enable minimally invasive delivery of extracellular matrix substitutes in vivo. Towards that goal, MAX1 is a 20 amino acid de novo designed peptide that undergoes triggered self-assembly to form a rigid hydrogel, Fig. 1 (Schneider et al. 2002). In slightly acidic aqueous solutions, MAX1 exists in an ensemble of random coil conformations rendering it fully soluble. The addition of an exogenous stimulus results in peptide folding into a 2:2 β-hairpin conformation (Sibanda and Thornton 1993) that undergoes rapid assembly into a highly crosslinked network. Thus, the ability of MAX1 to self-assemble into hydrogel is dependent on its intramolecularly folded conformational state. When properly folded, MAX1 self-assembles into hydrogel; when unfolded, the peptide is incapable of undergoing hydrogelation. Depending on the type of stimulus used to trigger folding and consequent self-assembly, material formation can be totally reversible (Pochan et al. 2003; Schneider et al. 2002). Simply removing the folding stimulus results in peptide unfolding and material dissolution.

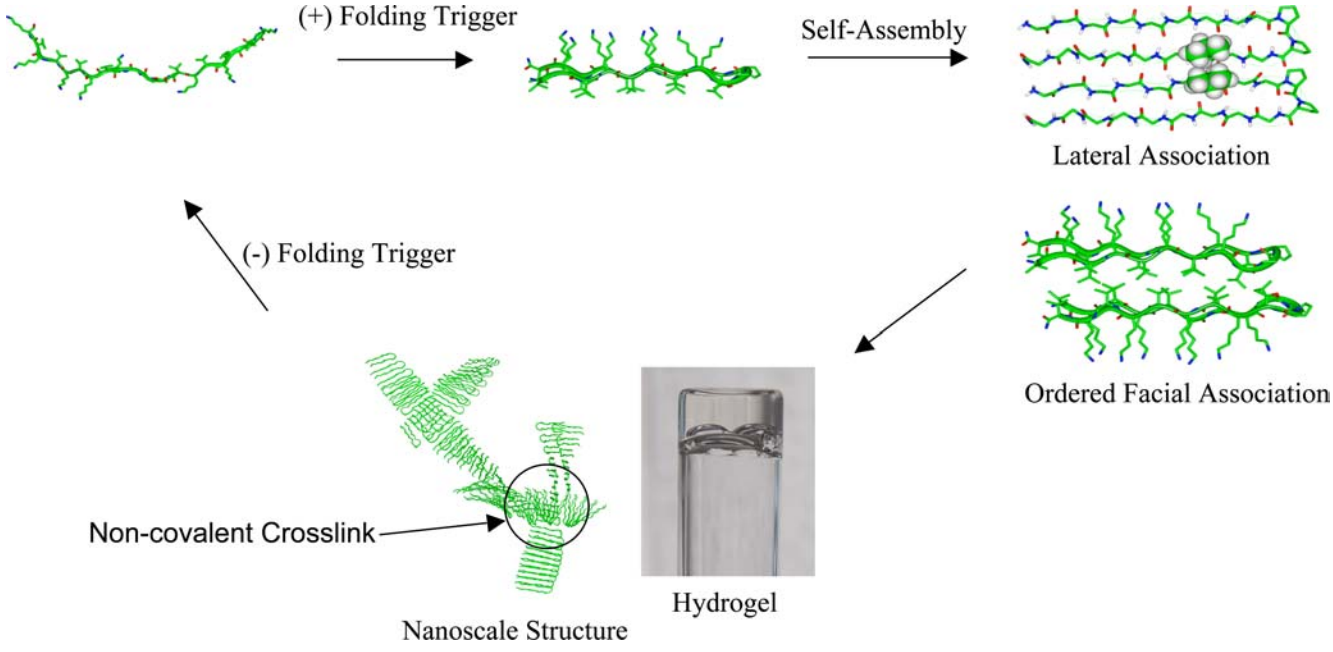

Fig. 1 Environmentally triggered folding, self-assembly and non-covalent fibril cross-linking leading to hydrogel formation. Crosslinks are formed by the irregular facial self-assembly of hairpins

MAX1 hydrogels are composed of more than 98% water and are microporous yet display significant rigidity as measured rheologically (Schneider et al. 2002). With respect to the hydrogel's utility in tissue engineering, cytocompatibility studies employing NIH 3T3 murine fibroblasts indicate that the gels are non toxic towards this model cell line (Kretsinger et al. 2005). Cells attach strongly to the hydrogel surface in the absence or presence of serum proteins and are able to proliferate to confluency with little effect on the gel's mechanical properties. Thus, MAX1 hydrogels meet the preliminary mechanical and cytocompatibility requirements of a tissue engineering scaffold (Lee and Mooney 2001).

MAX1 is composed of two β-strands, containing an alternating sequence of valine and lysine residues, connected by a beta turn, Fig. 2. The turn region consists of the tetrapeptide $-V^{D}PPT-$, a sequence designed to strongly promote type II' turn geometry (Chalmers and Marshall 1995; Favre et al. 1999; Nair et al. 1979); type II' turns are commonly found in β-hairpin motifs of naturally occurring proteins (Gunasekaran et al. 1997; Sibanda and Thornton 1985). The threonine residue at the $i+3$ position of the turn was included in the design since it has a high propensity to occupy this position in type II' turns of hairpins in naturally occurring proteins (Hutchinson and Thornton 1994). Threonine can form a stabilizing side chain-main chain H-bond between its alcoholic proton and the carbonyl oxygen of the ith residue of the turn. In the folded state, MAX1 displays a hydrophobic face composed mainly of valine residues and a hydrophilic face of lysine residues. One can take advantage of the lysine-rich face to trigger peptide folding and material formation. Under acidic conditions, the lysine side chains are protonated and charge repulsion between the strands of the hairpin inhibits folding. As a consequence, the peptide is highly soluble in aqueous media. When some of the side chain charge is alleviated, the peptide folds. This can be accomplished either by deprotonation of some of the lysines by adjusting the solution pH from acidic values to pH 9 under low ionic strength conditions (Schneider et al. 2002) or by screening existing charges at pH 7 by adjusting the ionic strength of the solution to physiological concentration (150 mM NaCl) (Ozbas et al. 2004a). In addition to manipulating electrostatic interactions, peptide folding is also governed by the formation of intramolecular Van der Waals (hydrophobic) contacts between residue side chains, the formation of intramolecular H-bonds between β-strands, as well as the turn propensity and hydrophobicity of the residues in the turn region.

Once folded, amphiphilic hairpins undergo both lateral and facial self-assembly. Lateral assembly occurs via the formation of intermolecular H-bonds and side chain–side chain hydrophobic contacts between assembling hairpins. Facial assembly occurs when the hydrophobic faces of assembling hairpins collapse to form a bilayer-like structure (Fig.1). The result of both lateral and facial assembly is the formation of a highly cross-linked network of short fibrils (10–200 nm) rich in β-sheet. TEM and SANS data (Ozbas et al., 2004b) support a model of assembly where fibrils are composed of a bilayer of intermolecularly H-bonded hairpins (Fig. 1). Intermolecular H-bonding occurs along the fibril axis reminiscent of cross β-structure. Bilayer formation within a given fibril can occur in an ordered fashion where the hydrophobic faces of individual hairpins stack

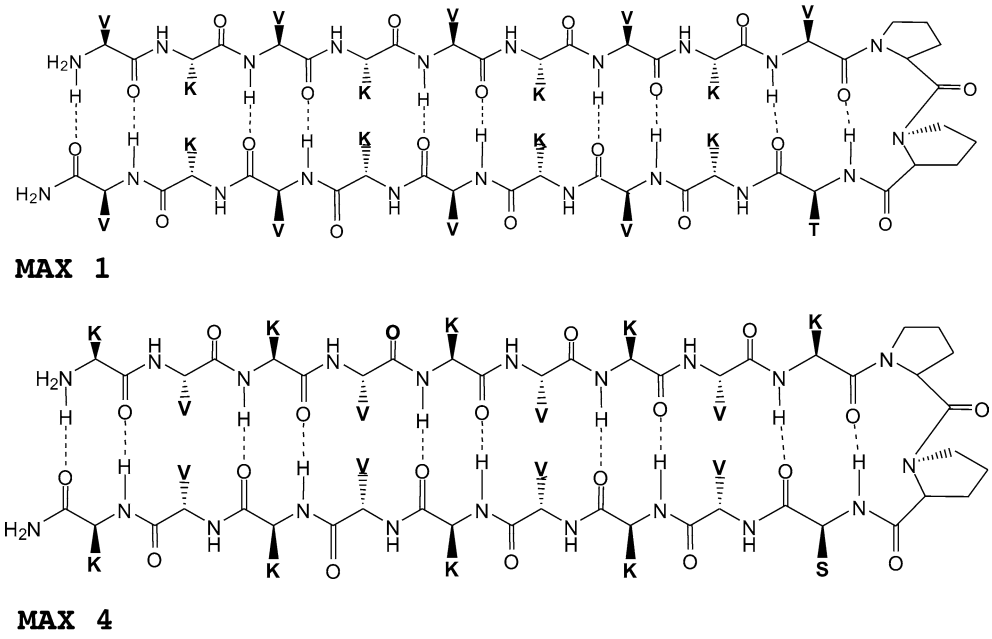

Fig. 2 β-hairpin structures of MAX 1 and MAX 4 as well as sequences of MAX1, MAX2, MAX4 and MAX5

MAX 1 : VKVKVKVKV^{D}PPTKVKVKVKV-CONH$_2$
MAX 2 : VKVKVKVKV^{D}PPTKVK**T**KVKV-CONH$_2$
MAX 4 : KVKVKVKVK^{D}PPSVKVKVKVK-CONH$_2$
MAX 5 : VKVKVKVKV^{D}PPSKVKVKVKV-CONH$_2$

directly on top of each other forming a well-defined laminate (Fig. 1). However, since the hydrophobic face of each hairpin is topologically smooth, irregular association also occurs where the face of one hairpin is rotated with respect to its partner in the bilayer; this provides a nucleation site for nascent fibril growth in a different direction, ultimately forming a non-covalently crosslinked network (Fig. 1).

Essential to both folding and self-assembly is the formation of intra- and intermolecular hydrophobic contacts, respectively. Interactions between non-polar groups in aqueous environments are known to be influenced by temperature (Murphy et al. 1990; Privalov 1990). In fact, we have shown that the folding and self-assembly of amphiphilic hairpins such as MAX1 can be triggered thermally (Pochan et al. 2003). At ambient temperatures, peptides are unstructured. However, on warming they adopt hairpin conformation and self-assemble into hydrogel. Increasing the temperature serves to dehydrate the nonpolar residues of the unfolded peptide and trigger folding via hydrophobic collapse (Badiger et al. 1998; Privalov 1988). Although this thermal folding/assembly transition is irreversible for MAX1, we have designed sequences that afford fully reversible transitions, e.g., warm the solution to induce folding and material formation; cool the hydrogel to unfold the peptide and disassemble/dissolve the material (Pochan et al. 2003).

Following the thermally dependent folding and self-assembly transitions of this class of hairpins by circular dichroism (CD) allows one to conveniently investigate the contribution of hydrophobic interactions to these processes. For example, the thermal folding/self-assembly transition for MAX2, a derivative of MAX1 where a valine at position 16 is changed to threonine, is shifted to higher temperature by about 15°C (Fig. 3). Although threonine is isostructural to valine, it is less hydrophobic; more thermal energy must be provided to dehydrate the nonpolar face of MAX2 as compared to MAX1 and as a result, the peptides fold and assemble at a higher temperature. Placing threonine at this position affects both facial and lateral self-assembly events since its side chain presumably makes contacts with both a hairpin

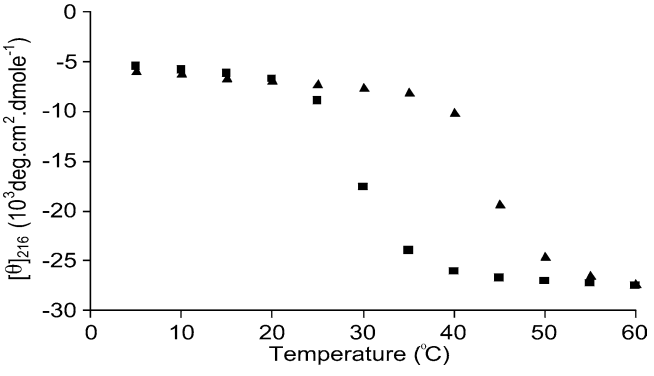

Fig. 3 Temperature dependent folding of MAX1(■) and MAX2(▲) at pH 9 (150 μM peptide, 125 mM borate and 10 mM NaCl). $[\theta]_{216}$ is measured as a function of temperature

above it in the bilayer and a hairpin beside it to which it is hydrogen bonded (Fig. 1).

In this paper, we probe the importance of making hydrophobic contacts during the lateral self-assembly event alone, as opposed to studying sequence changes that affect both facial and lateral assembly. In general, lateral assembly is governed by the formation of intermolecular H-bonds between the strands of distinct hairpins and the formation of lateral hydrophobic contacts between residue side chains of neighboring hairpins (Fig.1). The design of MAX1 includes placing valine residues at H-bonded positions within the primary sequence of each strand. Since valine prefers to adopt a *trans* χ_1 side chain rotamer when contained within β-sheet structure (Wouters and Curmi 1995), we anticipated that a large portion of MAX1 valine side chains would adopt *trans* dihedral angles. This places the methyl groups of the isopropyl side chains away from the center of the hairpin and extends these groups towards the valine side chains of neighboring hairpins (Fig. 4). The formation of valine-based lateral hydrophobic contacts via this mechanism should drive self-assembly and contribute to the rigidity of the hydrogel if these contacts help to stabilize the self-assembled state.

This hypothesis can be tested by designing a peptide that contains valine residues at non H-bonded positions (rather than H-bonded positions) within the strand regions of the hairpin. MAX4 contains the same number of residues as MAX1 and a similar turn region but contains β-strand sequences where valine residues occupy non H-bonded positions and lysine residues occupy H-bonded positions—exactly the opposite of MAX1. This simple change results in a hairpin whose hydrophobic and hydrophilic faces have been swapped as compared to MAX1 (Figs. 2 , 4). Because valine still prefers a *trans* χ_1 rotamer, the isopropyl side chains of MAX4 should extend towards the interior of the hairpin rather than the exterior as in MAX1 (Fig. 4). The change should not influence the ability of the hairpin to make facial hydrophobic contacts during assembly but should limit its ability to make lateral interactions. If forming lateral hydrophobic contacts contributes to MAX1 assembly and material properties, then MAX4 should display different properties such as diminished rates of self-assembly and form less rigid hydrogels as compared to MAX1. Importantly, the design of MAX4 necessitates that a polar residue occupy the $i+3$ position of the turn region since the side chain of this residue now extends towards the hydrophilic face of the hairpin. For MAX1, this face is hydrophobic and threonine normally occupies this position. MAX4 incorporates a serine at this position; serine is hydrophilic yet can still form the potentially turn-stabilizing side chain–main chain H-bond normally offered by threonine.

Lastly, the possibility exists that any changes in self-assembly and material properties observed for MAX4 could arise from simply replacing threonine with serine and not from altering any valine-based lateral interactions. MAX5, a control hairpin, was prepared that is nearly identical to MAX1 except that the threonine at position 12 is replaced with serine to study what effect this change has on folding, self-assembly and hydrogel rigidity in the absence of altering any possible lateral hydrophobic contacts.

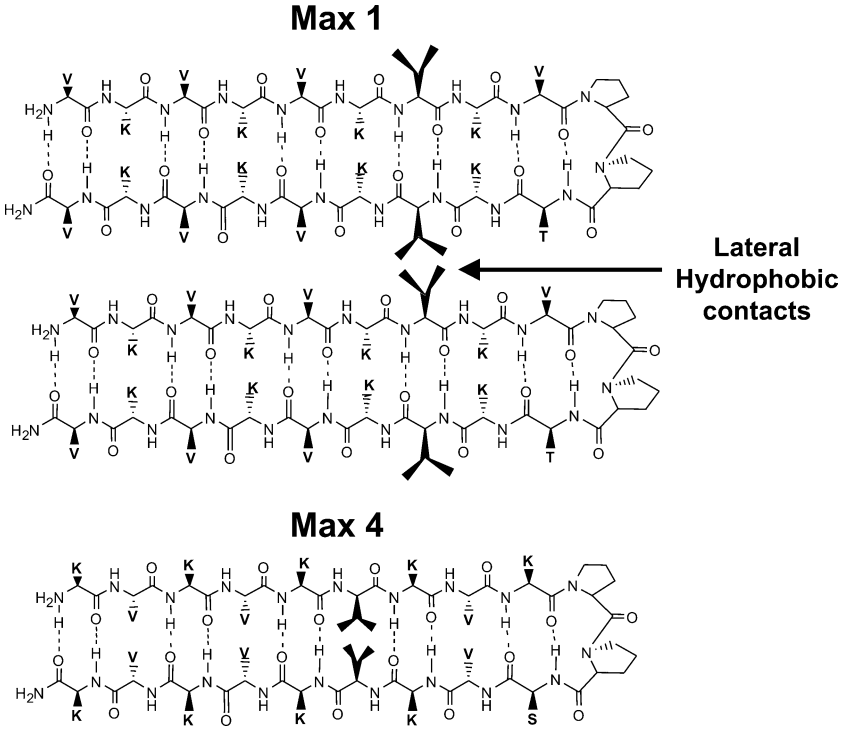

Fig. 4 Controlling intra and inter-molecular valine-based hydrophobic interactions. **a** Shows the hairpin structure of MAX1 with valines at hydrogen bonding positions. For valines at positions 7 and 14 the side chains are shown to demonstrate the formation of favorable intermolecular interactions between laterally assembled hairpins. **b** shows the hairpin structure of MAX4 with valines at non-hydrogen bonded positions; here, valine-based intermolecular interactions are designed against

Methods

All peptides were synthesized on Pal amide resin via automated Fmoc peptide synthesis employing an ABI 433A peptide synthesizer and HBTU/HOBT activation (Kretsinger and Schneider 2003). The resulting dry resin-bound peptides were cleaved and side-chain-deprotected using a cocktail of TFA, thioanisole, ethanedithiol and anisole in the ratio 90:5:3:2. Crude peptide was purified by RP-HPLC (preparative Vydac C18 peptide/protein column) employing a linear gradient from 12 to 100% B over 176 min, where solvent A is 0.1% TFA in water and solvent B is 90% acetonitrile, 10% water, and 0.1% TFA. Primary characterization of the peptides was accomplished by ESI mass spectrometry (see supplementary material).

Circular Dichroism spectra were collected on a Jasco J-810 spectropolarimeter. Three hundred micrometer stock solutions of each peptide in water were incubated in an ice bath as well as a concentrated pH 9 buffer solution (250 mM borate and 20 mM NaCl). Prior to the start of each experiment, equal volumes (125 μL) of the peptide stock and pH 9 buffer were gently mixed in a 1 mm quartz cell by cell inversion to yield the final peptide solution (150 μM peptide , 125 mM borate, 10 mM NaCl). The cell was immediately placed in the cell holder pre-equilibrated at 5°C. Temperature dependent wavelength scans were collected every 5°C with 10 min equilibration times at each temperature. For kinetic experiments, samples were prepared similarly at room temperature and immediately placed in the cell holder pre-equilibrated at 40°C. Data were collected at 216 nm at 5 second intervals for 15 min. Concentrations of peptide solutions were determined by absorbance at 220 nm ($\varepsilon =$ 15,750 cm^{-1} M^{-1}). Mean residue ellipticity [θ] was calculated from the equation $[\theta] = (\theta_{obs}/10lc)/n$, where θ_{obs} is the measured ellipticity (millidegrees), l is the length of the cell (centimeters), c is the concentration (molar), and n is the number (residues).

Oscillatory rheology: Dynamic time, frequency and strain sweep rheology experiments were performed on a stress controlled Physica MCR 500 rheometer with 25 mm diameter parallel plate geometry at 40°C. A 1 wt% sample was made by mixing equal volumes of peptide stock and pH 9.0 buffer solution at room temperature and transferred immediately to the rheometer. The dynamic time sweep experiment which measures the evolution of storage (G') and loss modulus (G'') with time was done for 1 h at constant strain (0.2%) and frequency (6 rad/s). This was followed by dynamic frequency sweep and strain sweep experiments on the same sample at 40 °C to establish the linear viscoelastic region.

Transmission electron microscopy: dilute samples of the peptides at 0.2% (w/v) were prepared in pH 9 buffer (125 mM borate, 10 mM NaCl) and equilibrated at 40°C for 10 min. Small amounts ($\sim$ 5 μL) of each hydrogel solution were applied to separate carbon coated copper grids. Excess solution was removed by filter paper after 1 min. The grid was then washed with deionized water (2×100 μL). Then, a 1 % (w/v) uranyl acetate aqueous solution was placed on each grid for negative staining and excess staining solution was blotted with filter paper and left to air dry. Bright field images of the samples were taken on a JEOL 2000-FX transmission electron microscope at 200 kV accelerating voltage with a Gatan CCD camera.

Bulk preparation of peptide hydrogels for general use can be accomplished by the following method that results in 300 μL of a 1 wt% gel; 3.0 mg of appropriate peptide was dissolved in 150 μL of Milli Q water to yield a clear solution and then 150 μL of pH 9 buffer stock solution (250 mM borate and 20 mM NaCl, pH 9.0) was added, resulting in a 1 wt % solution (pH 9.0, 125 mM borate and 10 mM NaCl) of peptide. After minimal pipet mixing, the solution is allowed to stand until gelation is complete.

Results and discussion

This class of amphiphilic peptides exhibit thermally-dependent folding and self-assembly transitions. For example, Fig. 5a shows CD spectra of dilute solutions (150 μM) of MAX1, MAX4 and MAX5 at 15 °C that indicate all three peptides are unfolded. Warming the solutions to 50 °C results in CD spectra indicative of β-sheet structure with clear minima centered at about 216 nm (Fig. 5b). All three hairpins afford spectra with similar absolute magnitudes of mean residue ellipticity suggesting that they all form assemblies with similar β-sheet content. At dilute peptide concentrations, such as those used in the CD experiments, there is not enough peptide to gel the aqueous solution. However, working at micromolar concentrations allows peptide folding and assembly to be followed spectroscopically because the resulting assemblies do not reach sizes capable of scattering light significantly. At higher concentrations (1 wt% = 3.07 mM), such as those used for rheological experiments, peptide assembly leads to complete gelation of the aqueous media.

We had previously determined that the exact temperature at which individual peptides fold and assemble (T_{gel}) is largely dependent on their hydrophobicity (Pochan et al. 2003). However, it was not clear whether T_{gel} is sensitive only to changes in overall residue side chain hydrophobicity or whether T_{gel} is also sensitive to how that hydrophobicity is specifically presented from the peptide backbone. In MAX1, hydrophobic valine side chains are arranged to maximize both facial and lateral interactions during self-assembly while in MAX4, these groups are arranged to make only facial contacts. Figure 5c shows that the temperatures at which MAX1 and MAX4 fold and assemble are nearly identical, with MAX4 being shifted slightly to higher temperatures. This shift is most likely due to the replacement of threonine with serine in the turn region. In fact, T_{gel} of the control peptide (MAX5), which is identical to MAX1

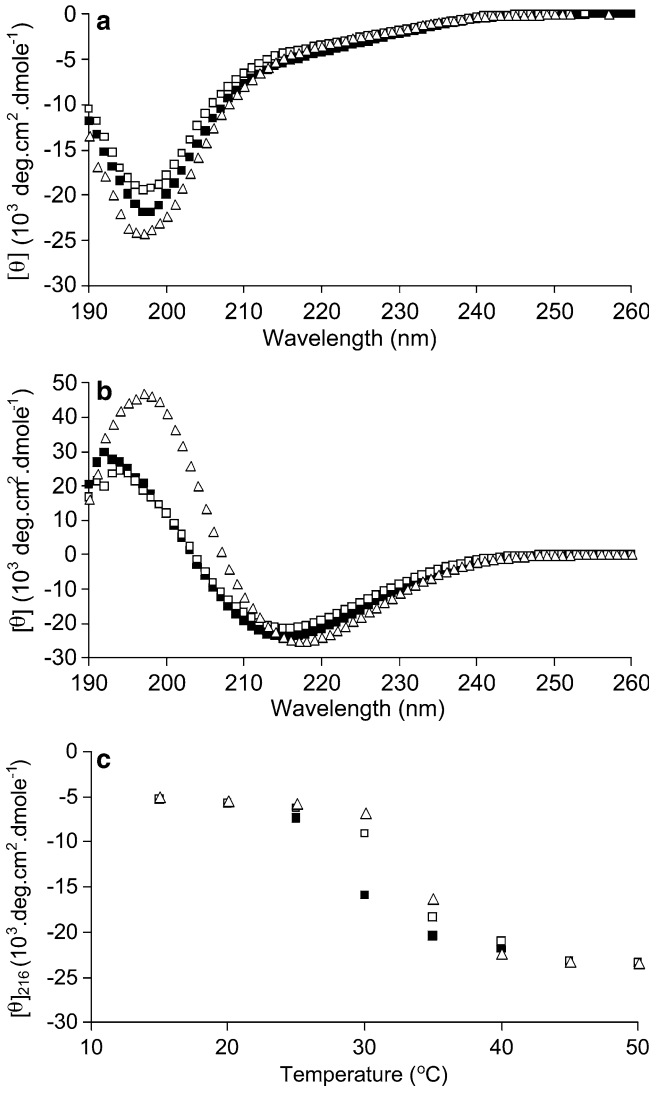

Fig. 5 Temperature dependent folding of MAX1 (■), MAX4 (△) and MAX5 (□) at pH 9 (150 μM peptide, 125 mM Borate, 10 mM NaCl). **a** Wavelength scans at 15°C show that all peptides are unfolded. **b** Wavelength scans at 50°C show that all peptides form β-sheet structure (c) $[\theta]_{216}$ measured as a function of temperature

except for the incorporation of serine at the same position, shifts to the same extent. These data suggest that the temperature at which folding and assembly is induced is largely independent of the exact spatial presentation of hydrophobic side chains as long as the overall amphiphilicity of the hairpin is conserved.

Although the exact spatial presentation of hydrophobes does not seem to affect T_{gel}, the kinetics of assembly are indeed affected. Figure 6 shows CD data where the mean residue ellipticity at 216 nm, an indicator of β-sheet formation, is monitored as a function of time after folding is initiated at 40 °C. Kinetics are conveniently measured at a common temperature that exceeds each peptide's T_{gel} (Fig. 5c) and ensures that MAX1, MAX4 and MAX5 reach a fully folded and assembled state. At 40 °C, MAX1 quickly folds and assembles, reaching apparent equilibrium after about 100 s. In contrast, MAX4 exhibits a clear attenuation in the initial rate of folding/assembly and reaches apparent equilibrium only after 250 s. This data suggests that the specificity of hydrophobic presentation influences the rate at which the peptide folds/assembles. However, the control peptide, MAX5 also exhibits slower kinetics as compared to MAX1. This indicates that replacing threonine with serine in the turn also negatively affects the kinetics, although to a much lesser extent.

Collectively, the CD data suggest that the formation of lateral hydrophobic contacts mediated by valine side chains contributes significantly to the rate of folding/self-assembly but does not necessarily play a role in dictating the temperature at which folding/assembly is triggered. Interestingly, Wouters and Curmi's statistical analysis of a non-redundant subset of proteins from the protein data bank indicates that valine residues have a propensity to exist in a pairwise fashion across β-strands. Importantly, there is a strong tendency for these residues to adopt trans side chain rotamers in order to facilitate close packing of the two valine side chains with each other in an interaction that the authors termed "nested packing" (Wouters and Curmi 1995). It is also possible that the slower sheet formation monitored by CD for MAX4 could be due to an alternate mode of facial packing during its assembly as compared to MAX1. However, both molecules contain only valine residues on their hydrophobic face resulting in uniformly smooth surfaces that should behave similarly. Although alternate modes of facial interactions cannot be ruled out, it is unlikely.

The exact nature of the lateral inter-valine interactions in the self-assembled state of MAX1 is currently unknown however, the contribution of this interaction to the mechanical properties of the hydrogel can be assessed by oscillatory rheology. Figure 7a shows time sweep data where storage moduli (G', a measure of the elastic response of the hydrogels) are measured for 1 wt% aqueous preparations of MAX1, MAX4 and MAX5 as a function of time after folding/assembly is triggered by warming the respective solutions to 40 °C.

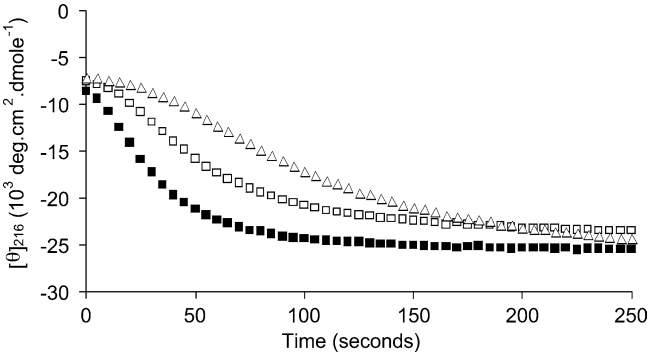

Fig. 6 Kinetics of β-sheet formation monitored at 40°C by measuring $[\theta]_{216}$ as a function of time for MAX1 (■), MAX4 (△) and MAX5 (□) at pH 9 (150 μM peptide, 125 mM Borate and 10 mM NaCl)

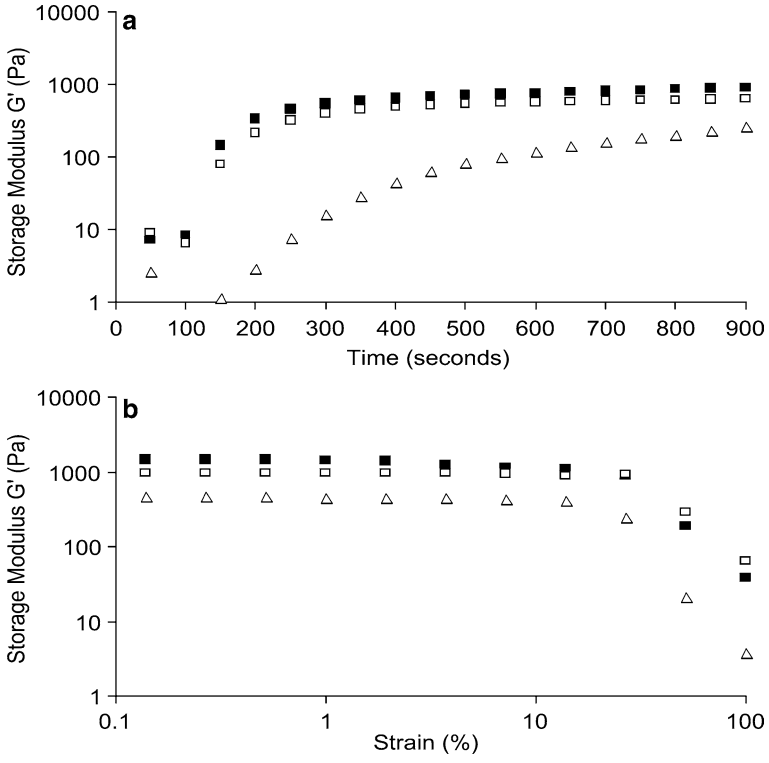

Fig. 7 Oscillatory rheology of 1 wt% MAX1 (■), MAX4 (△) and MAX5 (□) at pH 9. Hydrogelation is initiated by warming cool solutions to 40°C. **a** Dynamic time sweep experiment showing the evolution of storage modulus (G') with time at constant strain (0.2 %) and frequency (6 rad/s). **b** Dynamic strain sweep experiment showing linear viscoelastic region of each hydrogel. Material rigidity begins to breakdown at applied strains greater than 10%

The loss moduli (G'', a measure of the viscous response of the hydrogels) were also measured for each hydrogel (data not shown) and were at least an order of magnitude less than the storage moduli, exhibiting no crossover within 0.1–10 rad/s frequency range, indicating that all of the hydrogels form fairly rigid viscoelastic materials. The data shows that MAX1 quickly folds and assembles ultimately forming a hydrogel of considerable rigidity. The increase in storage modulus begins to plateau at 300 s and the hydrogel exhibits an equilibrium storage modulus of ~1,000 Pa at 900 s. In stark contrast, MAX4 exhibits a large lag in assembly kinetics and the resulting hydrogel is considerably less rigid (G' = 350 Pa at 900 s). Importantly, the control peptide, MAX5, assembles with comparable kinetics to that of MAX1 and the resulting hydrogel exhibits a storage modulus comparable to MAX1. This suggests that replacing threonine with serine in turn region of MAX4 has little effect and that the diminished rigidity of MAX4 hydrogel results from the inability of this hairpin to form efficient lateral hydrophobic contacts between valine residues in the self-assembled state. Figure 7b. shows strain sweep data where G' is measured as a function of applied strain. The percent strain at which the storage moduli sharply decrease is indicative of the material's brittleness. The structural integrity of all three hydrogels

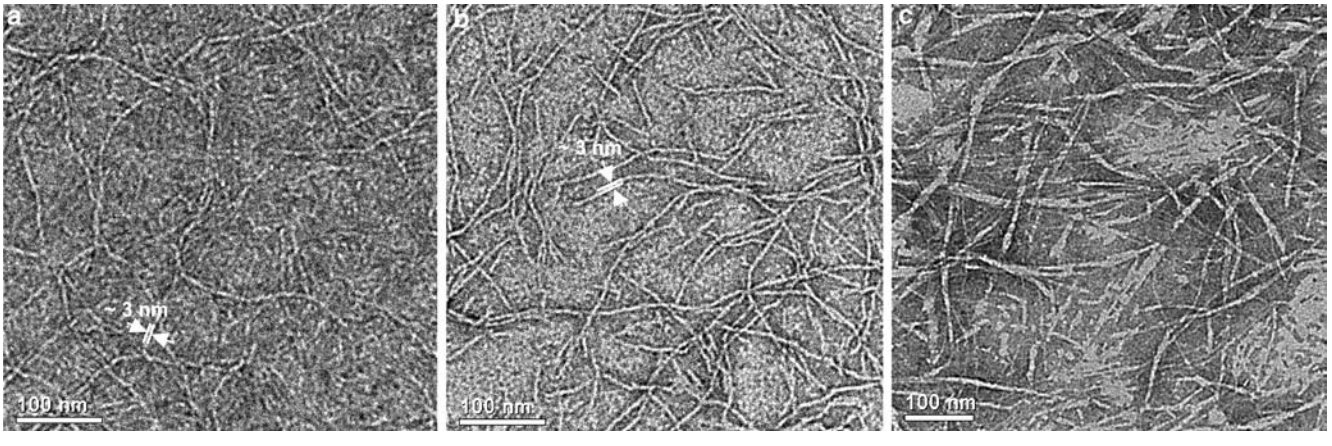

Fig. 8 Transmission electron micrographs of evaporated hydrogels showing nanoscale fibril morphology. **a** MAX1 forms single fibrils composed of an extended bilayer of assembled hairpins approximately 3 nm in diameter. **b** Control MAX5 forms similar fibrils that are approximately 3 nm in diameter. **c** MAX4 assembles into a mixture of single fibrils and tapes composed of fibrils that have undergone extensive higher order assembly. Scale bars are 100 nm

is compromised at strains greater than 10% with all exhibiting similar strain-responsive behavior.

Transmission electron micrographs of dilute gels (Fig. 8) that were dehydrated and negatively stained prior to imaging show that the positional placement of valine residues within the strands of the hairpin strongly influences the nano-scale morphology of the fibrils contained within the gel network. MAX1 and control MAX5 contain valines at H-bonded positions capable of engaging in intermolecular lateral association. Based on previous neutron scattering(Ozbas et al. 2004b) and congo red binding studies (data not shown) on MAX1; these hairpins most likely self-assembled laterally to form a hydrogen-bonded network along the length of the fibril reminiscent of cross beta structure. However, hairpins also self-assemble facially to bury their hydrophobic faces, forming an extended bilayer (a single laminate) along the length of a single fibril. Lateral and facial assembly results in single fibrils that are approximately 3 nm in diameter consistent with the length of the folded hairpin. These fibrils do not undergo any higher order assembly events (Fig. 8a, b). In contrast, Fig. 8c shows that MAX4, which contains valines at non-hydrogen bonded positions, assembles into single fibrils that are capable of engaging in higher order assembly events. Single fibrils and a mixture of tapes composed of assembled fibrils are clearly observed. Taken together, this data strongly suggests that the incorporation of valine residues at strand positions that allow lateral interactions between hydrophobic side chains of hairpins may be essential for well-defined fibril morphology.

Collectively, the data suggest that forming lateral hydrophobic interactions between valine side chains of assembling hairpins impacts the kinetics of folding/assembly as assessed by CD spectroscopy under dilute solution conditions. However, the temperature at which folding and assembly is initiated (T_{gel}) is little affected by the exact spatial presentation of these hydrophobic groups from the hairpin backbone. Importantly, at concentrations amenable to hydrogelation, the ability to form these lateral hydrophobic interactions directly impacts the rheological behavior of the peptide hydrogels; peptides capable of forming valine-based lateral contacts during assembly form more rigid gels faster. In addition, TEM shows that these interactions are essential in defining the nano-scale morphology of the fibrils that comprise the hydrogel network.

Acknowledgments This work was supported by the National Science Foundation (CHE0348323); the Physica MCR 500 rheometer was partly purchased with funds from the NIH (1-P20RR17716-01).

References

Aggeli A, Bell M, Boden N, Keen JN, Knowles PF, McLeish TCB, Pitkeathly M, Radford SE (1997) Responsive gels formed by the spontaneous self-assembly of peptides into polymeric beta-sheet tapes. Nature 386:259–262

Badiger MV, Lele AK, Bhalerao VS, Varghese S, Mashelkar RA (1998) Molecular tailoring of thermoreversible copolymer gels: Some new mechanistic insights. J Chem Phy 109:1175–1184

Chalmers DK, Marshall GR (1995) Pro-D-NMe-Amino Acid and D-Pro-NMe-Amino Acid: simple, efficient reverse-turn constraints. J Am Chem Soc 117:5927–5937

Collier JH, Hu BH, Ruberti JW, ZhangJ, Shum P, Thompson DH, Messersmith PB (2001) Thermally and photochemically triggered self-assembly of peptide hydrogels. J Am Chem Soc 123:9463–9464

Favre M, Moehle K, Jiang L, Pfeiffer B, Robinson JA (1999) Structural mimicry of canonical conformations in antibody hypervariable loops using cyclic peptides containing a heterochiral diproline template. J Am Chem Soc 121:2679–2685

Gunasekaran K, Ramakrishnan C, Balaram P (1997) b-hairpins in proteins revisited: lessons for de novo design. Protein Eng 10:1131–1141

Holmes TC (2002) Novel peptide-based biomaterial scaffolds for tissue engineering. Trends in Biotech 20:16–21

Hutchinson EG, Thornton JM (1994) A revised set of potentials for beta-turn formation in proteins. Prot Science 3:2207–2216

Kretsinger JK, Haines LA, Ozbas B, Pochan DJ, Schneider JP (2005) Cytocompatibility of self-assembled b-hairpin peptide hydrogel surfaces. Biomaterials 26:5177–5186

Kretsinger JK, Schneider JP (2003) Design and application of basic amino acids displaying enhanced hydrophobicity. J Am Chem Soc 125:7907–7913

Lee KY, Mooney DJ (2001) Hydrogels for tissue engineering. Chem Rev 101:1869–1879

Murphy KP, Privalov PL, Gill SJ (1990) Common features of protein unfolding and dissolution of hydrophobic compounds. Science 247:559–561

Nair CM, Vijayan M, Venkatachalapathi YV, Balaram P (1979) X-ray crystal structure of pivaloyl-D-pro-L-pro-L-ala-N-methylamide; observation of a consecutive b-turn conformation. J Chem Soc, Chem Commun pp 1183–1184

Ozbas B, Kretsinger J, Rajagopal K, Schneider JP, Pochan DJ (2004a) Salt-triggered peptide folding and consequent self-assembly into hydrogels with tunable modulus. Macromolecules 37:7331–7337

Ozbas B, Rajagopal K, Schneider JP, Pochan DJ (2004b) Semiflexible chain networks formed via self-assembly of b-hairpin molecules. Phys Rev Letters 93:268106/268101–268106/268104

Pochan DJ, Schneider JP, Kretsinger J, Ozbas B, Rajagopal K, Haines L (2003) Thermally reversible hydrogels via intramolecular folding and consequent self-assembly of a de novo designed peptide. J Am Chem Soc 125:11802–11803

Privalov PL (1988) Stability of protein-structure and hydrophobic interactions. Biol Chem Hoppe-Seyler 369:199

Privalov PL (1990) Cold denaturation of proteins. Crit Rev Biochem Mol Biol 25:281–305

Rajagopal K, Schneider JP (2004) Self-assembling peptides and proteins for nanotechnological applications. Curr Opin Struct Biol 14:480–486

Schneider JP, Pochan DJ, Ozbas B, Rajagopal K, Pakstis L, Kretsinger J (2002) Responsive hydrogels from the intramolecular folding and self-assembly of a designed peptide. J Am Chem Soc 124:15030–15037

Sibanda B, Thornton JM (1993) Accommodating sequence changes in b-hairpin in proteins. J Mol Biol 229:428–447

Sibanda BL, Thornton JM (1985) b-Hairpin families in globular proteins. Nature 316:170–176

Wouters MA, Curmi PMG (1995) An analysis of side-chain interactions and pair correlations within antiparallel beta-sheets - the differences between backbone hydrogen-bonded and non-hydrogen-bonded residue pairs. Proteins-Struct Functi Geneti 22:119–131

Zhang SG, Holmes TC, Dipersio CM, Hynes RO, Su X, Rich A (1995) Self-complementary oligopeptide matrices support mammalian-cell attachment. Biomaterials 16:1385–1393